Rabies Virus-induced Membrane Fusion Pathway

Yves Gaudin

Laboratoire de Génétique des virus du Centre National de la Recherche Scientifique (CNRS), 91198 Gif sur Yvette Cedex, France

Abstract. Fusion of rabies virus with membranes is triggered at low pH and is mediated by the viral glycoprotein (G). The rabies virus-induced fusion pathway was studied by investigating the effects of exogenous lipids having various dynamic molecular shapes on the fusion process. Inverted cone-shaped lysophosphatidylcholines (LPCs) blocked fusion at a stage subsequent to fusion peptide insertion into the target membrane. Consistent with the stalk-hypothesis, LPC with shorter alkyl chains inhibited fusion at lower membrane concentrations and this inhibition was compensated by the presence of oleic acid. However, under suboptimal fusion conditions, short chain LPCs, which were translocated in the inner leaflet of the membranes, considerably reduced the lag time preceding membrane merging, resulting in faster kinetics of fusion. This indicated that the rate limiting step for fusion is the formation of a fusion pore in a diaphragm of restricted hemifusion. The previously described cold-stabilized prefusion complex was also characterized. This intermediate is at a well-advanced stage of the fusion process when the hemifusion diaphragm is destabilized, but lipid mixing is still restricted, probably by a ring-like complex of glycoproteins. I provide evidence that this state has a dynamic character and that its lipid organization can reverse back to two lipid bilayers.

Key words: rhabdovirus • prefusion complex • liposome • viral fusion glycoprotein • lysophosphatidylcholine

Introduction

Entry of enveloped viruses into host cells requires fusion of the viral envelope with a cellular membrane. This step is mediated by virally encoded fusogenic glycoproteins. Activation of the fusion capacity involves structural rearrangement of these proteins upon interaction with specific triggers (e.g., low pH or specific receptors). It is generally assumed that these conformational changes result in the exposure of a fusion peptide or domain, which then interacts with and destabilizes one or both of the participating membranes.

Despite extensive work, mainly on influenza virus, the actual mechanism of the fusion process is still unknown. However, recent results have revealed striking similarities between different fusion systems. Experiments performed on viral or cellular membrane fusion have shown that inverted cone-shaped lysolipids (which promote a micellar positive spontaneous curvature) inhibit fusion when present in the contacting monolayers of membranes (Chernomordik et al., 1993, 1995; Vogel et al., 1993; Yeagle et al., 1994). These results have indicated that early lipidic fusion intermediates are similar from one system to another and that membrane fusion may proceed via the formation of stalk intermediates that are local lipidic connections with negative curvatures between contacting monolayers of fusing membranes (Siegel, 1993; Chernomordik et al., 1995). This step would be followed by the formation of a transient hemifusion diaphragm. Depending on the experimental system, hemifusion might be restricted (i.e., without lipid flux between both membranes) or unrestricted (i.e., without any restriction of lipid diffusion). Unrestricted hemifusion has been shown to be the final state of fusion mediated by engineered HA ectodomain anchored into the membrane by glycophosphatidylinositol (GPI-HA; Kemble et al., 1994; Melikyan et al., 1995b), whereas restricted hemifusion is encountered when HA-induced fusion is reversibly blocked at 4°C (Schoch et al., 1992; Chernomordik et al., 1998). Restriction of lipid flux has been suggested to be due to a ring-like aggregate of HA surrounding the hemifusion diaphragm (Chernomordik et al., 1998). Finally, complete fusion would occur by pore formation and enlargement in the hemifusion diaphragm (Melikyan et al., 1997; Chernomordik et al., 1998).

As the characteristics of the fusion pore and lipid dependence of fusion appear to be similar in all biological fusion events (Monck and Fernandez, 1992; Chernomordik et al.,

Address correspondence to Yves Gaudin, Laboratoire de Génétique des virus du CNRS, 91198 Gif sur Yvette Cedex, France. Tel.: 33 1 69 82 3837. Fax: 33 1 69 82 4308. E-mail:yves.gaudin@gv.cnrs-gif.fr

1995), this model for membrane fusion (i.e., stalk formation followed by hemifusion and pore formation) has been proposed to be universal. Although it is also supported by theoretical considerations on energetics of lipidic structures (Siegel, 1993), this model is mainly based on experiments performed on influenza virus hemagglutinin (HA)[1] (Chernomordik et al., 1997, 1998) and remains to be challenged in other fusion systems.

Rabies virus-induced membrane fusion is mediated by the viral transmembrane glycoprotein (G) which is organized in trimers (three monomers of 65 kD each; Whitt et al., 1991; Gaudin et al., 1992). The fusion properties of rabies virus have been investigated (Gaudin et al., 1993). Fusion is triggered at low pH, optimal around pH 5.8–6, and is not detected above pH 6.3. Fusion of rabies virus with liposomes is preceded by a lag time, the duration of which increases with lower temperature and higher pH (up to the pH threshold for fusion). Preincubation of the virus below pH 6.75 in the absence of a target membrane leads to inhibition of viral fusion properties. However, this inhibition is reversible and readjusting the pH to above 7 leads to the complete recovery of the initial fusion activity. This is the main difference between rhabdoviruses (such as rabies virus) and other viruses fusing at low pH for which low pH-induced fusion inactivation is irreversible (Gaudin, 2000).

Low pH-induced conformational changes of the glycoprotein and their relationships with fusion activity have been studied. It has been demonstrated that G can assume at least three different states (Gaudin et al., 1993): the native (N) state detected at the viral surface (pH 7); the activated (A) hydrophobic state; and the fusion inactive conformation (I). There is a pH-dependent equilibrium between these states that is shifted toward the I state at low pH. The A state is detected immediately after acidification, induces the formation of viral aggregates stabilized at low pH and low temperature (Gaudin et al., 1993), and interacts with the target membrane as a first step of the fusion process (Durrer et al., 1995). The I state is detected after prolonged incubation at low pH. In the I conformation, G is longer than in the N conformation, but also antigenically distinct and more sensitive to proteases. The exact role of I during the fusion process is unclear, but it has been proposed that the role of the I state is to avoid fusion during transport of G in the acidic Golgi vesicles (Gaudin et al., 1995). For vesicular stomatitis virus (VSV), another rhabdovirus, the same three states have been postulated on the basis of kinetics studies (Clague et al., 1990; Puri et al., 1992).

The domain of rhabdoviral G interacting with the target membrane (the so-called fusion peptide) has been located using hydrophobic photolabeling (Durrer et al., 1995) and by directed mutagenesis (Li et al., 1993; Zhang and Ghosh, 1994; Fredericksen and Whitt, 1995, 1996). These results have suggested that an uncharged domain of VSV G from amino acid 118 to 136 and the homologous domain of rabies virus constitute the fusion peptide of the glycoprotein.

Recent structural studies of the fusion glycoprotein of influenza virus, retroviruses, Ebola virus, and Simian Virus 5 (a paramyxovirus) have indicated remarkable similarities (Bullough et al., 1994; Fass et al., 1996; Chan et al., 1997; Weissenhorn et al., 1997, 1998; Baker et al., 1999; Kobe et al., 1999). All these fusion protein ectodomains form rod-shaped α-helical bundles. In the structural studies, both the COOH-terminal membrane anchor and the NH_2-terminal fusion peptide were removed (to have a soluble molecule), but the results strongly suggest that these peptides are colocated at one end of the rod (Skehel and Wiley, 1998). As it has been demonstrated for the HA, this conformation is not the metastable native conformation of the fusion protein, but most probably represents the structure of this protein at the end of the fusion process. A common feature of all these fusion glycoproteins is that they are synthesized as a precursor that must be cleaved to generate the NH_2-terminal fusion peptide. This is not the case for rhabdoviruses for which there is no activating cleavage of the fusion protein. Furthermore, no coiled-coil formation is predicted for the rhabdovirus glycoprotein and a careful look over the amino acid sequence of G does not reveal any obvious heptad repeats. These observations, together with the reversibility of the low pH-induced conformational changes, suggest that rhabdoviral G may define another category of fusogenic proteins and thus, is a good candidate to challenge the proposed model for membrane fusion.

In the present study, using a liposome assay, I have investigated the sensitivity of rabies virus-induced membrane fusion to lysophosphatidylcholine (LPC) having aliphatic chains of varying length, and to oleic acid (OA). The results are consistent with the fusion model proposed for influenza virus (Chernomordik et al., 1998). The data also indicate that under suboptimal fusion conditions the rate limiting step for membrane fusion is the formation of a fusion pore in a diaphragm of restricted hemifusion. Furthermore, the lipidic structure in the previously described cold-stabilized prefusion complex (Gaudin et al., 1993; Durrer et al., 1995) was characterized. It appeared that this intermediate is at an advanced stage of the fusion process when a putative hemifusion diaphragm is already destabilized, but lipid mixing is still restricted, most probably by a ring-like complex of glycoproteins. This state has a dynamic character and its lipid organization can reverse back to two lipid bilayers. Finally, although the data support the idea that the lipidic fusion intermediates are the same for influenza and rabies virus-induced membrane fusion, they also reveal some subtle differences that will be discussed and have to be taken into consideration for a global understanding of virus-induced membrane fusion.

Materials and Methods

Chemicals

N-(lissamine rhodamine B sulfonyl)-phosphatidylethanolamine (RHO-PE), *N*-(7-nitro-2,1,3-benzoxadiazol-4-yl)-phosphatidylethanolamine (NBD-

[1]*Abbreviations used in this paper:* FIF, frozen intermediate of fusion; G, rabies virus glycoprotein; GPI-HA; HA ectodomain linked to glycosylphosphatidylinositol; HA, influenza virus hemagglutinin; LPC, lysophosphatidylcholine; NBD-PE, *N*-(7-nitro-2,1,3-benzoxadiazol-4-yl)-phosphatidylethanolamine; OA, oleic acid; PC, phosphatidylcholine; PE, phosphatidylethanolamine; RHO-PE, *N*-(lissamine rhodamine B sulfonyl)-phosphatidylethanolamine; RVPC, rabies virus prefusion complex; TMRD-3000, tetramethylrhodamine dextran with a molecular mass of 3,000.

PE), 1-lauroyl-2-hydroxy-sn-glycero-3-phosphocholine (lauroyl LPC), 1-myristoyl-2-hydroxy-sn-glycero-3-phosphocholine (myristoyl LPC), 1-palmitoyl-2-hydroxy-sn-glycero-3-phosphocholine (palmitoyl LPC), and 1-stearoyl-2-hydroxy-sn-glycero-3-phosphocholine (stearoyl LPC) were purchased from Avanti Polar Lipids, Inc. Phosphatidylcholine (PC; type III-B from bovine brain), phosphatidylethanolamine (PE; type I from bovine brain), gangliosides (type III from bovine brain), OA, calcein, and tetramethylrhodamine coupled to dextran with a molecular mass of 3,000 (TMRD-3000) were supplied by Sigma-Aldrich, and L-3-phosphatidyl [*N*-methyl-^{3}H]choline 1,2-dipalmitoyl ([^{3}H] PC) was supplied by Amersham Pharmacia Biotech.

Virus Purification

The PV (Pasteur Vaccine) strain was grown in BSR cells (clone of baby hamster kidney 2l cells) at 37°C in MEM supplemented with 2% calf serum. Virus particles were purified from the culture supernatant 72 h postinfection. In brief, cell debris were first eliminated by a 30-min centrifugation at 3,500 rpm in a JA14 rotor (Beckman Coulter) at 4°C. The virus was then pelleted by centrifugation at 4°C (3 h at 14,000 rpm in a JA14) and resuspended in TD buffer (137 mM NaCl, 5 mM KCl, 0.7 mM Na_2HPO_4, 25 mM Tris-HCl, pH 7.5). Viral purification was achieved by another centrifugation of 50 min through 30% glycerol in 10 mM Tris-HCl, pH 7.5, 50 mM NaCl, 1 mM EDTA at 25,000 rpm in a SW 28 (Beckman Coulter) at 4°C.

Preparation of Liposomes and Assay for Fusion

A total of 700 μg of PC, 300 μg of PE, and 100 μg of gangliosides dissolved in organic solvents were mixed with 10 μg of RHO-PE and 10 μg of NBD-PE and dried in vacuo. The lipidic film was suspended in 1 ml of buffer A (150 mM NaCl, 5 mM Tris-HCl, pH 8) and the mixture was bath-sonicated for 20 min. Liposomes were used within 3 d.

Fusion was assayed as previously described by using the resonance energy transfer method of Struck et al. (1981). If not indicated otherwise, all fusion experiments were performed at 22°C. 10 μl of fluorescent liposomes were mixed with 980 μl of phosphate-citrate buffer at the required pH (prepared from 100 mM citric acid and 200 mM dibasic sodium phosphate solution) in the cuvette of a thermostated Perkin-Elmer LS50B spectrofluorimeter. Then, 10 μl of virus (~50 μg of viral proteins) was added and the increase of NBD fluorescence was monitored continuously. In this range of viral concentrations, the increase of NBD fluorescence was proportional to the viral concentration and thus to the number of fusion events. Excitation was at 455 nm (slit width, 4 nm) and emission was at 535 nm (slit width, 10 nm). The mixture was kept under continuous stirring during the experiments.

For studies on the prefusion complex, 10 μl of virus (50 μg of viral proteins) were incubated with 10 μl of liposomes and 20 μl of phosphate-citrate buffer, pH 6.45, on ice for the indicated duration, and the mixture was diluted in the spectrofluorimeter cuvette in 960 μl of phosphate-citrate buffer at the required pH.

Experiments performed with the same viral stocks, same liposome preparations, and same buffers were highly reproducible (fusion extent variations were <5%). However, the extent and kinetics of fusion under suboptimal pH conditions (pH 6.2) were variable when different viral stocks, liposomes preparations, or buffer (pH buffer could vary within ± 0.02 pH units) were used. Experiments presented here were repeated at least three times and all qualitative results reported in this paper were observed in each experiment.

Leakage Measurements

Calcein was encapsulated into liposomes by hydrating the lipid film in buffer containing 40 mM calcein, 80 mM NaCl, 2 mM EDTA, 5 mM Tris-HCl, pH 8 (calcein was dissolved by addition of ~120 mM NaOH in the buffer). TMRD-3000 was encapsulated by hydrating the lipid film in buffer A containing 20 mg/ml of the dye. After sonication, free dyes were removed by molecular sieve chromatography on sephadex G-75 equilibrated with buffer A (containing 2 mM EDTA when calcein was used). Relief of self-quenching due to dilution of the dye upon leakage was measured by monitoring calcein fluorescence at 520 nm with excitation at 490 nm (slit width 2.5 nm) and TMRD-3000 fluorescence at 580 nm with excitation at 530 nm (slit width 5 nm). The measurements were carried out in buffer A (containing 2 mM EDTA when calcein-loaded liposomes were used). The initial fluorescence intensity of TMRD-3000 or calcein-loaded liposomes was set to zero.

Inhibition of Fusion By LPC and OA

Stock solutions of lauroyl (5 mM), myristoyl (1 mM), and palmitoyl (1 mM) LPC were freshly prepared as aqueous dispersions. Stock solution of stearoyl LPC (1 mM) and OA (1 mM) were freshly prepared as ethanolic solutions. In fusion experiments, the lipids were added into the cuvette containing the liposomes diluted in phosphate-citrate buffer at the required pH 2 min before addition of the virus. This time was largely sufficient to reach the equilibrium of their partition between the aqueous medium and the liposome membrane as judged by the increase of NBD fluorescence (due to exogenous lipid incorporation), which had reached a plateau after a few seconds (see Fig. 2 A).

The increase of NBD fluorescence due to lipid incorporation into the liposomes was used to estimate the amount of lipid incorporated. To evaluate how various dilutions of NBD-PE and RHO-PE affect the extent of NBD-PE fluorescence, a 1:1 (wt/wt) mixture of NBD-PE and RHO-PE was diluted into different amounts of a 7:3:1 (wt/wt/wt) mixture of PC, PE, and gangliosides in organic solvents. Liposomes were then made as described in the previous paragraph. Fluorescence of NBD was measured before (F) and after (F_0) 0.8% Triton X-100 addition. A plot of F_0/F versus the fluorescent probe dilution gave a calibration curve that was used to estimate the incorporation of lipids in the liposomes. This approach assumes that the fluorescent probes and the added lipids are homogeneously and independently distributed in the liposome membrane.

Liposome Binding to Virus

For these experiments, liposomes were made as described above, but contained 40 μCi of [^{3}H] PC per mg of lipid. For binding experiments, 15 μl of liposomes were mixed with 75 μl of phosphate-citrate buffer at pH 6.45 or 150 mM NaCl, 50 mM Tris-HCl, pH 8, and 10 μl of virus (50 μg of viral proteins). The mixture was incubated for 3 min on ice, layered onto a cold 25% glycerol solution in 150 mM NaCl, 50 mM Tris-HCl, pH 8, or in phosphate-citrate buffer pH 6.45, and then centrifuged for 30 min at 40,000 rpm in an SW55 rotor (Beckman). The amount of liposomes associated with virus in the pellet was determined by liquid scintillation counting. To study their effect on liposome binding to virus, exogenous lipids were added to the mixture before addition of the virus.

Results

Effect of LPC on Rabies Virus-induced Membrane Fusion

Altering membrane lipid composition by addition of lipids that affect the curvature of lipid monolayers has been used to study the different stage of membrane fusion (Chernomordik et al., 1993, 1997; Vogel et al., 1993; Yeagle et al., 1994). Of particular interest are the inverted cone-shaped LPC that promote a micellar positive spontaneous curvature, and the cone-shaped cis-unsaturated fatty acids that promote inverted hexagonal H_{II} phase. Thus, stalk formation should be promoted by cis-unsaturated fatty acids and inhibited by LPC when these lipids are present in the outer leaflet of the membranes. On the other hand, pore formation and expansion should be promoted by LPC and inhibited by cis-unsaturated fatty acids when these lipids are present in the inner leaflet of the membranes (Chernomordik et al., 1998).

The dependence of fusion on the presence of various concentrations of LPC with saturated aliphatic chains of varying lengths (from 12 to 18 hydrocarbon groups) was studied. Under optimal fusion conditions (pH 5.85), the extent of fusion decreased in a dose dependent manner (Figs. 1 and 2 D). The LPC concentrations used in these experiments did not solubilize the liposomes: as shown in Fig. 2 A, upon LPC addition, an increase of NBD fluorescence was observed that was much slighter than the increase of NBD fluorescence upon addition of solubilizing

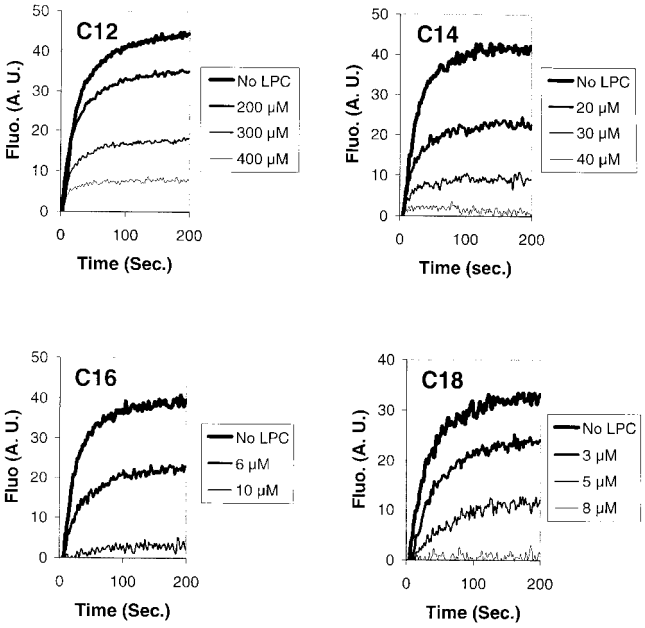

Figure 1. Inhibition of rabies virus-induced fusion by LPC under optimal fusion conditions. Fusion was assayed at pH 5.85 and 22°C. Effects of increasing concentrations of lauroyl (C12), myristoyl (C14), palmitoyl (C16), and stearoyl (C18) LPC on fusion between rabies virus and fluorescent liposomes containing NBD-PE and RHO-PE. The increase of NBD fluorescence was measured as described in Materials and Methods. Fluo., Fluorescence; A.U., arbitrary units.

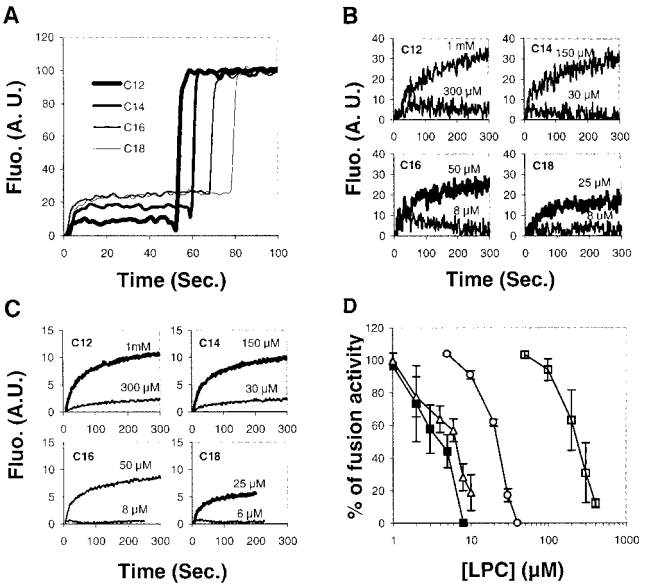

Figure 2. A, Concentrations of LPC that inhibit fusion do not solubilize liposomes. 10 μl of fluorescent liposomes were mixed with 990 μl of buffer A in the cuvette of the spectrofluorimeter. The initial fluorescence intensity of NBD was set to zero. Lauroyl (C12; 300 μM), myristoyl (C14; 30 μM), palmitoyl (C16; 8 μM), or stearoyl (C18; 8 μM) LPC were added (at t = 0 s) in the cuvette. When the equilibrium was reached, membranes were solubilized with Triton X-100 (0.8%). The increase of NBD fluorescence after Triton X-100 addition was normalized to 100. B, LPC-induced leakage of calcein-loaded liposomes. Liposomes (final concentration, 10 μg/ml of phospholipids) were mixed with buffer A (supplemented with 2 mM EDTA) in the cuvette of the spectrofluorimeter. The initial fluorescence intensity of calcein was set to zero and lauroyl (C12), myristoyl (C14), palmitoyl (C16), or stearoyl (C18) LPC were added (at t = 0 s) in the cuvette at the indicated concentrations. C, LPC-induced leakage of TMRD-3000–loaded liposomes. Liposomes (final concentration, 10 μg/ml of phospholipids) were mixed with buffer A in the cuvette of the spectrofluorimeter. The initial fluorescence intensity of TMRD-3000 was set to zero and lauroyl (C12), myristoyl (C14), palmitoyl (C16) or stearoyl (C18) LPC were added (at t = 0 s) in the cuvette at the indicated concentrations. D, Inhibition of rabies virus-induced fusion by LPC under optimal fusion conditions. The extent of fusion at pH 5.85 and 22°C, assayed by the increase of NBD fluorescence, was plotted versus the total concentration of lauroyl (□), myristoyl (○), palmitoyl (△), and stearoyl (■) LPC in the medium. The 100% fusion activity was measured in absence of LPC. The graph shows the mean of five experiments like the one shown in Fig. 1. Error bars indicate SD.

concentrations of Triton X-100 (0.8%). This slight increase of NBD fluorescence was due to incorporation of LPC into the membrane of the liposomes resulting in dilution of RHO-PE and NBD-PE, and consequently in a decrease of the transfer energy efficiency.

Potential leakage induced by LPC was also investigated. For palmitoyl (C16) and stearoyl (C18) LPC, no leakage was observed when fusion-inhibiting concentrations were used. For these lysolipids, three to four times higher concentrations than those used in the inhibition experiments were necessary for the encapsulated dyes to leak out (Fig. 2, B and C). A slight leakage of TMRD-3000, occurring much slower than in the presence of solubilizing concentrations of LPC, was detected when fusion-inhibiting concentrations of lauroyl (C12) and myristoyl (C14) LPC were used (Fig. 2 C). This leakage was not detected when calcein-loaded liposomes were used (although calcein is smaller than TMRD-3000), but slight increase of calcein fluorescence could have been hidden by the noisy signal (Fig. 2 B). Taken together, these control experiments indicated that the inhibitory effect of LPC was neither due to solubilization nor to lysis of liposomes.

As in other systems (Chernomordik et al., 1997), the inhibiting concentrations were dependent on the length of the hydrocarbon chains: LPC with longer chains have an inhibiting effect at lower concentrations (Figs. 1 and 2 D, Table I). However, as it is well documented that partitioning of LPCs into membranes increases with their hydrophobicity (i.e., with their hydrocarbon chain length), the concentration of LPC in the membranes was evaluated using NBD dequenching (due to LPC incorporation into the membrane), and the calibration curve was obtained as described in Materials and Methods. Estimates of the membrane concentrations required to cause 50% inhibition of fusion are indicated in Table I. It appeared that LPC with shorter hydrocarbon chains (and thus a more pronounced inverted cone shape) required lower membrane concentrations to inhibit fusion.

Under suboptimal fusion conditions (pH 6.2), palmitoyl (C16) and stearoyl LPC (C18) were still inhibiting fusion in a dose dependent manner at concentrations similar to those inhibiting fusion at pH 5.85 (Fig. 3). However, al-

Table I. Total and Membrane LPC Concentrations Giving 50% Fusion Inhibition

LPC	Total LPC concentration giving 50% fusion inhibition	Membrane concentration of LPC giving 50% fusion inhibition
	μM	%
Lauroyl	240 ± 50	4.1 ± 0.5
Myristoyl	23 ± 2	5.8 ± 0.5
Palmitoyl	6.5 ± 1	8.7 ± 2
Stearoyl	4.1 ± 2	9.9 ± 2

The total LPC concentration in the medium giving 50% of fusion inhibition was calculated from the graph in Fig. 2. The amount of LPC incorporated in the membrane, and thus the membrane concentration of LPC giving 50% of inhibition, were calculated as indicated in Materials and Methods.

though still inhibiting fusion at high concentrations, lauroyl (C12) and myristoyl (C14) LPC increased the number of fusion events at low concentrations (Fig. 3). Furthermore, in the presence of lauroyl and myristoyl LPC, the lag time preceding fusion at pH 6.2 disappeared and the initial kinetics of fusion were faster.

The simplest explanation of these first results is that incorporation of LPC in the outer leaflet of the membranes resulted in inhibition of stalk formation as demonstrated by the results obtained at pH 5.85. Furthermore, Fujii et al. (1985) have shown that the rate of transbilayer movement of LPC increases with decreasing acyl chain length (consistently with the slight leakage of liposomes observed in the presence of lauroyl and myristoyl LPC; Fig. 2 C), the results obtained at pH 6.2 strongly suggest that lauroyl and myristoyl LPC, but not palmitoyl or stearoyl LPC, were translocated in the inner leaflet and thus were present in both monolayers. Indeed, the presence of lauroyl and myristoyl LPC in the inner leaflet would promote pore formation and expansion, and would explain the increase in fusion extent, together with the faster kinetics of fusion. Finally, at pH 6.2, the lag time preceding fusion was no longer detected in the presence of lauroyl and myristoyl LPC. This indicates that this lag time is not due to slow binding of the virions to the liposomes, but rather that the rate limiting step of fusion under suboptimal conditions is the formation and the expansion of a fusion pore in a hemifusion diaphragm.

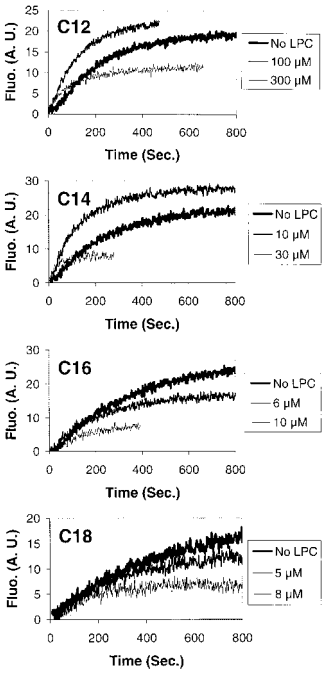

Figure 3. Inhibition and promotion of rabies virus-induced fusion by LPC under suboptimal fusion conditions. Fusion was assayed at pH 6.2 and 22°C. Effects of increasing concentrations of lauroyl (C12), myristoyl (C14), palmitoyl (C16), and stearoyl (C18) LPC on fusion between rabies virus and fluorescent liposomes containing NBD-PE and RHO-PE. The increase of NBD fluorescence was measured as described in Materials and Methods. Fluo., Fluorescence; A.U., arbitrary units.

LPC Does Not Inhibit Fusion Peptide Insertion in the Target Membrane

Although the inhibiting effect of LPC on rabies virus-induced membrane fusion could be explained by their effect on the outer monolayer curvature, it was also possible that part of their inhibiting action was due to binding to the hydrophobic fusion peptide which could then no longer insert into the target membrane. Such a mechanism for LPC-induced fusion inhibition has been proposed for the case of HIV gp120/gp41-mediated fusion (Günther-Ausborn and Stegmann, 1997).

Thus, a potential inhibition of rabies virus binding to target liposomes was investigated. For this, rabies virus was incubated for three minutes at pH 6.45 and 0°C with liposomes containing tritiated PC in the presence of LPCs. Under these conditions, although no fusion is detected, the virions interact in a hydrophobic manner with the target membrane via their fusion peptides. These conditions previously have been defined as prefusion conditions (Gaudin et al., 1993; Durrer et al., 1995). After incubation, the mixture was centrifuged through a 30% glycerol cushion, above which unbound liposomes were floating, and the radioactivity associated with the virus in the pellet was assayed by liquid scintillation counting. The results are presented in Fig. 4. They show that the presence of 300 µM lauroyl, 30 µM myristoyl, 10 µM palmitoyl, or 10 µM stearoyl LPC was without effect on virus binding to the liposomes, indicating that it was indeed their ability to induce a micellar positive curvature of the outer leaflet, which was responsible for their ability to inhibit fusion.

Effect of OA on Rabies Virus-induced Membrane Fusion

The effect of cone-shaped lipids on fusion was then studied, and liposomes were incubated with various OA concentrations before addition of the virus. The effect of OA was dependent on pH. At pH 6.2, OA inhibited the fusion reaction. A concentration of 5 µM OA decreased the ex-

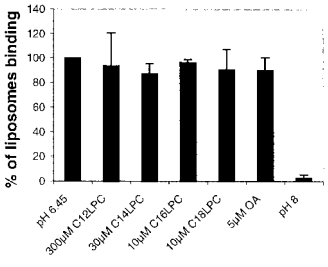

Figure 4. Exogenous lipids do not inhibit insertion of the fusion peptide in the target membrane. Virions were incubated for 3 min on ice with tritiated liposomes at pH 8 or at pH 6.45 in absence or in the presence of the indicated exogenous lipids concentration. The mixture was centrifuged as described in Materials and Methods, and the amount of liposomes associated with virus in the pellet was determined by liquid scintillation counting. The graph shows the mean of three independent experiments. Error bars indicate SD. The value of radioactivity associated with the virus at pH 6.45 in absence of exogenous lipids was defined as 100%, and the other values were calculated as percentages thereof.

tent of fusion by a factor of 2.5 and a concentration of 10 μM virtually completely inhibited fusion (Fig. 5, pH 6.2). At lower pH, OA was much less inhibiting, and at pH 5.85 (Fig. 5), a concentration of 20 μM of OA was without effect on the fusion reaction. Potential inhibition of virus–liposome binding by OA was also assayed. Again (Fig. 4) it was shown that under prefusion conditions, OA was without effect on virus binding to the liposomes. Thus, as OA is known to be easily translocated in the inner leaflet (Broring et al., 1989), inhibition of the fusion reaction under suboptimal fusion conditions was probably due to inhibition of pore formation and expansion in the hemifusion diaphragm.

Compensation of the Inhibiting Effect of LPC by Addition of OA

The inhibiting effect of LPC at pH 5.85 could be compensated at least partially by addition of OA into the membranes (Fig. 6). The compensatory effect was stronger with palmitoyl and stearoyl LPC (Fig. 6, B and C), but was still detected with myristoyl LPC (Fig. 6 A). No compensatory effect of OA on fusion inhibition by lauroyl LPC was observed. However, presence of OA affected the incorporation of lauroyl LPC into the membranes as judged by the larger increase of NBD fluorescence (data not shown).

These results are in agreement with the additivity of lipid effects on the spontaneous curvature of lipid monolayer (Madden and Cullis, 1982), and reinforce the idea that the inhibiting effect of LPC is due to its ability to induce a positive curvature of the outer membrane leaflet.

Structure of the Prefusion Complex

As mentioned above, we have previously demonstrated the existence of a stable prefusion complex (Gaudin et al., 1993; Durrer et al., 1995) that is formed when the virus is preincubated between pH 6.3 and 6.7 with liposomes on ice. The kinetics of formation of the rabies virus prefusion complex (RVPC) at pH 6.45 and 0°C were investigated (Fig. 7). Virions were incubated for increasing periods in the presence of liposomes at pH 6.45 and 0°C. The mixture was then diluted in the spectrofluorimeter cuvette containing a pH 6.2 phosphate-citrate buffer at 22°C. In the absence of this preincubation step, the fusion curve at pH 6.2 and 22°C had a typical sigmoidal shape and the increase of NBD fluorescence was preceded by a lag time of ~30 s (Fig. 7, but also see Fig. 2). Preincubation of the virus with the liposomes at pH 6.45 and 0°C resulted in faster fusion kinetics, disappearance of the lag time, and increase of fusion extent. A significant modification of the aspect of the fusion curve was already detected after a 20 s preincubation (Fig. 7), and the effect was maximal after ~2 min as longer preincubations did not result in faster fusion kinetics or larger increase of fusion extent (data not shown).

As LPCs were able to arrest fusion after hydrophobic interaction of the glycoprotein, but before lipid mixing, it was interesting to test the effect of LPC on fusion once RVPC is made. For this, virions were incubated with lipo-

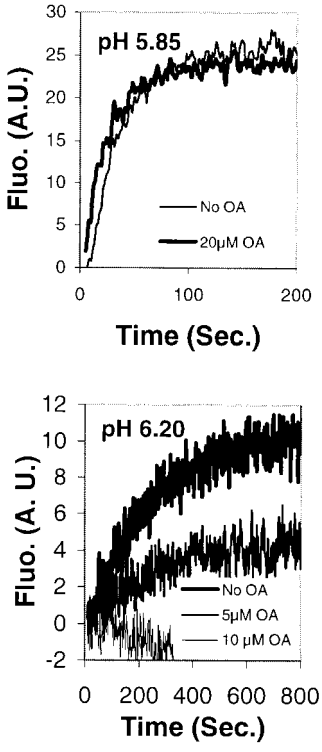

Figure 5. Inhibition of rabies virus-induced fusion by OA under suboptimal fusion conditions. Effects of increasing concentrations of OA on fusion between rabies virus and fluorescent liposomes containing NBD-PE and RHO-PE at pH 5.85 and pH 6.2. The increase of NBD fluorescence was measured as described in Materials and Methods. Fluo., Fluorescence; A.U., arbitrary units.

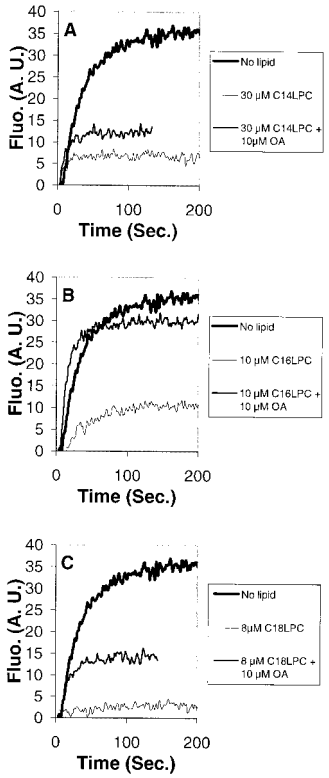

Figure 6. LPC and OA compensate the effects of each other on rabies virus-induced fusion. Fusion was assayed at pH 5.85 and 22°C. Myristoyl (A), palmitoyl (B), and stearoyl (C) LPC were added at the indicated concentrations into the cuvette containing the liposomes 1 min before addition of OA and 2 min before addition of the virus. The increase of NBD fluorescence was measured as described in Materials and Methods. Fluo., Fluorescence; A.U., arbitrary units.

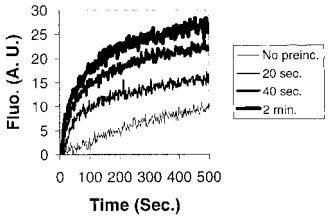

Figure 7. Kinetics of formation of the prefusion complex. Fusion was assayed at pH 6.2 and 22°C after preincubation of the virus with the liposomes at pH 6.45 and 0°C for the indicated durations, as described in Materials and Methods. Fluo., Fluorescence; A.U., arbitrary units.

somes at 0°C, either at pH 6.45 or 7.4 for three minutes. The prefusion complex was made at pH 6.45, but not at pH 7.4. The mixture was then diluted in the spectrofluorimeter cuvette containing phosphate-citrate buffer at pH 5.85 in the presence or absence of 10 μM LPC (palmitoyl or stearoyl LPC). After a preincubation of the virions and the liposomes at pH 7.4, lipid mixing was still sensitive to LPC (Fig. 8, pH 7.4), whereas when the prefusion complex was previously formed at pH 6.45 and 0°C, lipid mixing was then largely insensitive to LPC (Fig. 8, pH 6.45). The results of these experiments indicated that at pH 6.45 and 0°C, fusion is blocked at a stage downstream of the palmitoyl and stearoyl LPC-sensitive stage.

Finally, the disappearance of the lag time at pH 6.20 indicates that once RVPC is made, most of the events preceding lipid mixing have already occurred. As experiments performed with lauroyl and myristoyl LPC have indicated that the rate limiting step of the fusion process at pH 6.2 could be the formation of a fusion pore and its expansion in a hemifusion diaphragm, this suggests that at pH 6.45 and 0°C, fusion is blocked at a well-advanced stage when a putative hemifusion diaphragm is already destabilized, but lipid mixing is still restricted.

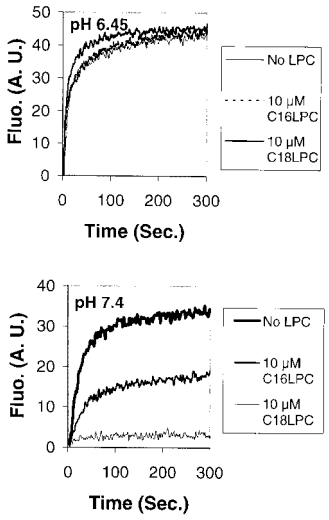

Figure 8. In RVPC, fusion is blocked at a stage subsequent to the LPC-sensitive stage. Virions and liposomes were incubated for 3 min on ice at pH 6.45 or 7.4 before dilution in the spectrofluorimeter cuvette containing phosphate-citrate buffer at pH 5.85 in the absence or presence of 10 μM palmitoyl or stearoyl LPC. The prefusion complex was made at pH 6.45, but not at pH 7.4. Fluo., Fluorescence; A.U., arbitrary units.

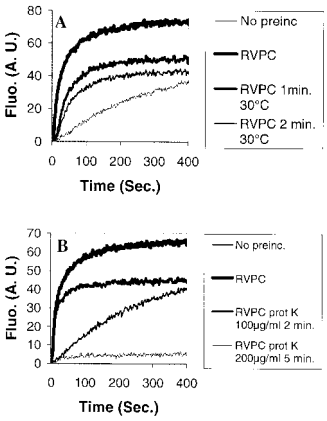

Figure 9. A, RVPC is disrupted by incubations at pH 6.45 and 30°C. Virions and liposomes were incubated for 3 min on ice at pH 6.45. The mixture was then diluted directly (RVPC), or after a 1- or 2-min incubation at 30°C (RVPC 1 min 30°C; RVPC 2 min 30°C, respectively), in the spectrofluorimeter cuvette containing phosphate-citrate buffer at pH 6.2 and 22°C. The last curve (No preinc.) corresponds to fusion at pH 6.2 and 22°C in absence of a preincubation with the liposomes at pH 6.45 on ice. B, RVPC is disrupted by proteinase K treatment. Virions and liposomes were incubated for 3 min on ice at pH 6.45. The mixture was then diluted directly (RVPC) or after a proteinase K treatment at pH 6.45 and 0°C as indicated, in the spectrofluorimeter cuvette containing phosphate-citrate buffer at pH 6.2 and 22°C. The last curve (No preinc.) corresponds to fusion at pH 6.2 and 22°C in absence of a preincubation with the liposomes at pH 6.45 on ice.

Merger of Membranes Inside RVPC Is Reversible

As already demonstrated (Gaudin et al., 1993; Durrer et al., 1995), a second protonation step lowering the pH below 6.3 is necessary to induce the transition from the RVPC state to complete fusion. Indeed, incubation of RVPC at pH 6.45 and temperature above 20°C did not induce any increase of NBD fluorescence (data not shown). Furthermore, after incubation of RVPC at pH 6.45 and 30°C (Fig. 9 A), the rate and the extent of fusion induced at pH 6.2 were lower than the rate and extent observed when RVPC was directly diluted at pH 6.2 (i.e., when virions and liposomes were only preincubated for three minutes at pH 6.45 and 0°C), indicating a progressive disruption of RVPC under such conditions.

Similar results were obtained when RVPC was treated with proteinase K at pH 6.45 and 0°C (Fig. 9 B). Thus, proteolysis of G also resulted in breaking RVPC without inducing complete fusion (as a control, dilution of RVPC in the fluorimeter cuvette thermostated at 0°C containing phosphate-citrate buffer at pH 6.45 and proteinase K did not induce any fluorescence increase).

These results indicate that the transition from RVPC to complete fusion is still a glycoprotein-dependent process and that local membrane merger (and maybe even initial pore formation in a restricted hemifusion diaphragm) is not sufficient to allow spontaneous complete fusion of membrane lipid bilayers. The corollary is that fusion pore expansion is still a high-cost energy step.

As disruption of RVPC resulted in the lipid organization reversing back to two lipid bilayers, it was interesting to see the effect of prolonged incubation of RVPC at pH 6.45 and 0°C in the presence of LPC. In fact, since LPC should not support the curvature adopted by the external lipid monolayer in RVPC, LPC should dissociate the connections between the outer leaflets of target and viral membranes. This was indeed the case as incubation of RVPC for 30 s in the presence of palmitoyl LPC significantly decreased the rate and the extent of fusion induced at pH 6.2, and longer incubations (15 min) resulted in complete fusion inactivation (Fig. 10 A). It was important to control that this effect was not due to slow glycoprotein extraction from viral particles. For this purpose, virus and liposomes were incubated with the same concentration of palmitoyl LPC as in Fig. 10 A for 10 min. This treatment resulted in complete inhibition of fusion after dilution of the mixture in the cuvette (final pH was 6.1; Fig. 10 B, curve LPC). However, when BSA was added to the mixture before triggering fusion, the integrity of the fusion activity was recovered (Fig. 10 B, curve LPC + BSA). This indicated that BSA was able to extract LPC from the membranes and that no LPC-induced solubilization of the viral glycoproteins occurred during the experiment.

As a conclusion, in RVPC, although fusion is blocked at a stage downstream of the LPC-sensitive stage (Fig. 8), the

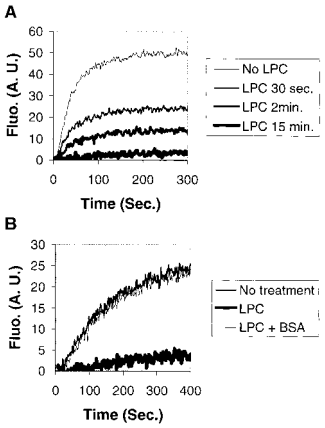

Figure 10. A, RVPC is disrupted by prolonged incubation in the presence of LPC. Virions (50 μg of viral proteins) and liposomes were incubated for 3 min on ice at pH 6.45. The mixture was then diluted in 150 mM NaCl (final volume 500 μl, concentration of phospholipids 20 μg/ml) containing palmitoyl LPC (final concentration 25 μM) and kept on ice for indicated times before a two-time dilution in the spectrofluorimeter cuvette containing phosphate-citrate buffer pH 6.2 at 22°C (in the cuvette the concentration of liposomal phospholipids and of palmitoyl LPC was 10 μg/ml and 12.5 μM, respectively). As a control (No LPC), the mixture of virions and liposomes was diluted in 150 mM NaCl containing no LPC and kept on ice for 15 min before dilution in the spectrofluorimeter cuvette. B, LPC does not extract glycoproteins from viral membrane. Virions (50 μg of viral proteins) and liposomes were mixed in buffer A (final volume 500 μl, concentration of phospholipids 20 μg/ml) in the absence (No treatment) or presence (LPC) of palmitoyl LPC (final concentration 25 μM) and kept on ice for 10 min before a two-time dilution in the spectrofluorimeter cuvette containing phosphate-citrate buffer pH 6.1 at 22°C. The last curve (LPC + BSA) corresponds to virions and liposomes mixed in buffer A, kept on ice for 10 min in the presence of palmitoyl LPC, and subsequently incubated on ice with BSA (2.5 mg/ml) for 10 min before a two-time dilution in the spectrofluorimeter cuvette containing phosphate–citrate buffer pH 6.1 at 22°C.

lipid organization is still sensitive to prolonged incubations in the presence of LPC. This reveals the dynamic character of this fusion intermediate and confirms that this stage can still reverse back to two membranes.

Discussion

Lipids of different shape, such as lysolipids or cis-unsaturated fatty acids, have proved to be useful tools to study the structural intermediates occurring during the fusion process (Chernomordik et al., 1993, 1995, 1997, 1998; Vogel et al., 1993; Yeagle et al., 1994). In the present study, I have used LPC and OA to determine the rabies virus-induced fusion pathway. The effects of these lipids on rabies virus-induced fusion are similar to those observed in other fusion systems and reinforce the idea that the fusion pathway is the same in all biological fusion events.

LPC Incorporated in the Outer Leaflet of Membranes Inhibits Rabies Virus-induced Membrane Fusion Consistently with the Stalk Hypothesis

Under optimal fusion conditions (pH 5.85), LPCs with aliphatic chains having 12–18 hydrocarbon groups inhibit fusion in a range of inhibitory concentrations in solution that is similar to that observed for the influenza virus (Chernomordik et al., 1997). This result is in agreement with the predictions of the stalk model for fusion as presence of LPC in the outer leaflet would inhibit stalk formation (Chernomordik et al., 1999). However, the mechanism of LPC inhibition of fusion is often debated. Particularly, one alternative interpretation is that LPC directly binds to the fusion peptide of fusogenic glycoproteins and inhibits its interaction with the target membrane (Günther-Ausborn and Stegmann, 1997). The results presented here rule out this hypothesis for rabies virus as the presence of LPC does not inhibit virus binding to liposomes under prefusion conditions. Furthermore, addition of OA was found to compensate the inhibitory effect of LPC in agreement with its complementary cone shape. This result indicates that it is membrane-incorporated LPC rather than LPC in solution that is responsible for fusion inhibition. Finally, as for the influenza virus, it appears that although the aqueous concentration of lauroyl LPC giving a twofold inhibition is ~60 times higher than that of stearoyl LPC, the corresponding membrane concentration of lauroyl LPC is two times lower than that of stearoyl LPC. As lauroyl LPC has a more pronounced inverted cone shape, here again, this result is consistent with the stalk hypothesis.

In the case of influenza virus-induced fusion, presence of OA in the outer leaflet of the fusing membranes promoted fusion, presumably because it promoted stalk formation (Chernomordik et al., 1997). Interestingly, rabies virus-induced fusion was not promoted in the presence of OA (except when LPC was added previously in the membranes). This suggests that stalk formation is an efficient process in this fusion system, which cannot be further enhanced by presence of OA in the outer leaflet. This difference with the influenza virus may be due to intrinsic properties of the fusion machinery of both viruses. However, it may also be due to the different experimental procedures, as Chernomordik et al. (1997) were working with cells expressing HA fusing with red blood cells, whereas I used viruses fusing with liposomes. Both the density of fusogenic glycoproteins (much higher at the viral surface) and different constraints on cellular and liposomal membranes may explain this difference of efficiency in stalk formation.

Rabies Virus Induced-membrane Fusion Proceeds Via the Formation of a Lipidic Pore in a Hemifusion Diaphragm

Another critical issue for fusion mediated by a protein machinery is the nature of the fusion pore: is it a proteinaceous pore whose expansion leads to lipid merger (Lindau and Almers, 1995) or a lipidic pore in a hemifusion diaphragm (Zimmerberg et al., 1993; Kemble et al., 1994; Melikyan et al., 1995b, 1997; Chernomordik et al., 1998)? In general, inhibition of fusion by membrane-incorporated LPC is considered as a strong argument in favor of the latter hypothesis (Chernomordik et al., 1998, 1999), but two other observations presented here are also consistent with a lipidic nature of the fusion pore.

First, under suboptimal fusion conditions, OA, which is known to be translocated in the inner leaflet (Broring et al., 1989), inhibits fusion as expected from a cone-shaped lipid promoting negative curvature of the inner leaflet. Second, one striking and unexpected result was the disappearance of the lag time preceding fusion and the faster kinetics of fusion in the presence of lauroyl and myristoyl LPC under suboptimal fusion conditions (pH 6.20). This demonstrates

that the events preceding membrane continuity were sensitive to the shape of the lipids present in the membranes. Thus, the lag time detected before the onset of fusion was not due to slow binding of the virions to the liposomes, but rather to slow reorganization of the lipids in the fusion complex. The faster fusion kinetics were not observed with LPC having longer hydrocarbon chains. As the rate of transbilayer movement of LPC increases with decreasing acyl chain length (Fujii et al., 1985) consistently with the results presented here on LPC-induced leakage, this suggests that lauroyl and myristoyl LPC were translocated in the inner leaflet and, in agreement with the lipidic pore model, would promote pore formation in a hemifusion diaphragm. Thus, the fusion enhancement observed at low concentrations of lauroyl and myristoyl LPC under suboptimal conditions is probably due to an increased proportion of hemifusion diaphragms that transformed into complete fusion although less stalks were made. Finally, the disappearance of the lag time in the presence of lauroyl and myristoyl LPC indicates that the rate limiting step for fusion under suboptimal conditions would be the formation of a fusion pore and its enlargement into a hemifusion diaphragm.

In the Prefusion Complex, the Hemifusion Diaphragm Is Already Destabilized, but Lipid Mixing Is Still Restricted

Previously, we had demonstrated that when viruses and liposomes are preincubated at slightly acidic pH (between pH 6.4 and 6.7) and 0°C, although no membrane continuity is detected, rabies virions bind to the liposomes in a hydrophobic manner and their fusion peptides are inserted in the target membrane (Gaudin et al., 1993; Durrer et al., 1995). Here, the structure of this RVPC was investigated.

The results indicated that once RVPC is made, most of the events preceding membrane continuity are already achieved. In fact, arguments presented in the results section suggest that in RVPC, fusion is blocked at an advanced stage when a fusion pore is already present in the hemifusion diaphragm, but lipid mixing is still restricted.

Restriction of lipid diffusion was first demonstrated in HA-induced membrane fusion (Chernomordik et al., 1998). This restriction is supposed to be due to the formation of a ring-like complex made of several low pH-activated HA (Blumenthal et al., 1996; Danieli et al., 1996). In the case of the rhabdoviruses, it has been shown that more than one trimer of G is required to build a competent fusion site (Bundo-Morita et al., 1988; Gaudin et al., 1993). Furthermore, we have recently described two rabies mutants with mutations in their glycoprotein for which the conformational change toward the inactivated state is considerably slowed down. Interestingly, these mutants presented an unexpected phenotype: they showed a hexagonal lattice of G at their surface under prefusion conditions (pH 6.6 and 0°C). Each angle of a hexagon seemed to be made up by a trimer of G and the lattice was not observed when spikes in the inactivated conformation were detected (Gaudin et al., 1996). We have proposed that one hexagon, once associated with a target membrane, constitutes a minimal prefusion complex for rabies virus (Gaudin et al., 1999). If this is true, diffusion of the lipids inside this hexagon might be restricted either by the transmembrane domains or by membrane-inserted fusion peptides of the activated glycoproteins making up a hexagon. The fact that, in photolabeling experiments performed under prefusion conditions (6.4 and 0°C), labeling was found only in the fusion peptide and not in the transmembrane domain (Durrer et al., 1995) suggests that lipid diffusion is restricted by fusion peptides inserted in the target membrane. This could also be the case for influenza virus because GPI-HA lacking HA transmembrane domain has been shown to induce restricted hemifusion under suboptimal fusion conditions (Chernomordik et al., 1998).

The properties of RVPC resemble those of the so-called frozen intermediate of fusion (FIF; also called committed state) observed for influenza HA-induced fusion (Schoch et al., 1992; Chernomordik et al., 1998). However, it has been shown that FIF is a restricted hemifusion that precedes fusion pore formation (Chernomordik et al., 1998), whereas the kinetics presented here suggest that pore formation has already occurred in RVPC. In fact, the lipidic organization in RVPC is probably similar to the structure of the flickering pore observed in influenza virus-induced fusion (Melikyan et al., 1993, 1995a; Tse et al., 1993; Zimmerberg et al., 1994), which is also a dynamic intermediate.

Reversibility of Membrane Merger at the RVPC-arrested Stage

In the case of influenza HA-induced membrane fusion, once FIF is made, fusion can be achieved at pH 7.4 and 37°C. This is not the case with RVPC for which a second protonation step (occurring below pH 6.3) is absolutely required for fusion to be triggered. In fact, increasing the temperature without lowering the pH simply results in slow disruption of RVPC and progressive recovery of the sigmoidal shape of the fusion curves when fusion is further induced at pH 6.2 and 23°C. It could be tempting to relate this result to the reversibility of the rhabdovirus glycoprotein conformational changes (Crimmins et al., 1983; Doms et al., 1987; Puri et al., 1988, 1992; Clague et al., 1990; Gaudin et al., 1991, 1993; Pak et al., 1997). However, as treatment of RVPC by proteinase K also results in RVPC disruption without inducing any fusion, this indicates that the transition from RVPC to complete fusion is a high-cost energy step that depends on the integrity and the correct refolding of the glycoproteins directly involved in the fusion process. This also rules out the hypothesis that local membrane connections are sufficient to allow spontaneous fusion of lipid bilayers in agreement with recent results obtained by Leikina and Chernomordik (2000) using influenza HA to induce membrane fusion. Finally, together with the fact that prolonged incubation of RVPC with LPC at pH 6.45 and 0°C also resulted in its disruption, proteolysis experiments also demonstrate that the lipid organization in RVPC can reverse back to its initial state (i.e., two bilayers) and that the energy cost of local membrane merger in RVPC is compensated by the energy provided by G conformational changes.

Toward a Universal Model for Fusion

Despite the important differences between their fusion machineries (Gaudin, 2000), rabies virus and influenza vi-

rus-induced membrane fusion follow a similar pathway (Fig. 11). In both cases, the first step in the fusion process is the insertion of the fusion peptide into the target membrane (Stegmann et al., 1991; Tsurudome et al., 1992; Durrer et al., 1995) and maybe also into the viral membrane (Weber et al., 1994; Wharton et al., 1995). This insertion would induce the formation of a stalk structure that connects target and viral membranes. The initial stalk structure would then expand and the inner leaflets of the membranes would form a hemifusion diaphragm. This step would be followed by pore formation and expansion leading to complete fusion. This fusion model is also supported by data obtained from other fusion systems: stalk formation is consistent with the lysolipid-induced inhibition of calcium-triggered exocytosis, GTP dependent fusion of rat liver microsomes, pH-induced fusion of insect cells infected by baculovirus, and Sendai virus fusion with liposomes (Chernomordik et al., 1993, 1995; Yeagle et al., 1994). Hemifusion has been detected not only in the case of fusion induced by GPI-HA (Kemble et al., 1994; Melikyan et al., 1995b), but also in the case of fusion induced by HA having a mutation in position 1 of HA_2 (Qiao et al., 1999), and in the case of paramyxovirus SV5 fusion protein lacking its intraviral COOH-terminal domain (Bagai and Lamb, 1996). Finally, for both the influenza and rabies virus, complete fusion is preceded by a stage at which lipid diffusion is strongly restricted. This step seems to involve a ring-like structure made up of activated fusogenic glycoproteins. Such a structure is also encountered in the case of baculovirus GP64-induced membrane fusion (Plonsky and Zimmerberg, 1996; Markovic et al., 1998) suggesting that the supramolecular organization of the fusion machinery is similar from one system to another.

Although the mechanism of membrane rearrangements leading to fusion is probably universal, depending on the experimental conditions, fusion may be blocked at different stages that are not the same from one system to another. For example, the membrane organization is probably not the same in RVPC and FIF, as RVPC seems to be at a more advanced stage on the fusion pathway. Thus, dissecting the fusion pathway of various fusion systems and identifying stable intermediates will certainly be useful if one wants to get a detailed cinematic view of the fusion mechanism and to know how proteins induce this complex process.

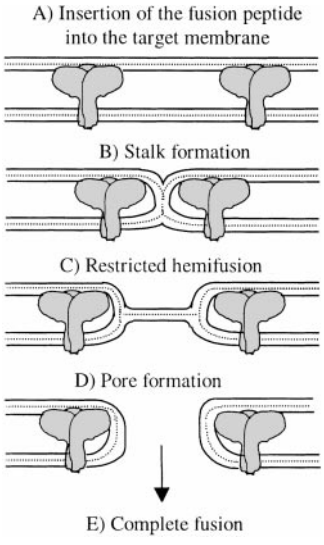

Figure 11. Rabies virus-induced fusion pathway. A, The initial low pH-induced conformational change results in exposition of the glycoprotein fusion peptide that interacts with the target membrane. B, The result of this insertion is the formation of a stalk that connects the outer leaflets of the fusing membranes inside a ring of glycoproteins. Stalk formation is inhibited by LPC present in the outer leaflet. C, This is followed by the formation of a hemifusion diaphragm in which lipid diffusion is restricted. D, The next step is the formation of a fusion pore in the hemifusion diaphragm. Lipid diffusion is still restricted. This is the stage arrested at pH 6.45 and 0°C (RVPC). At this stage, the lipid organization can still reverse back to two membranes. E, Another step of protonation would break the ring of glycoproteins and would induce membrane fusion.

I am greatly indebted to Leonid Chernomordik for valuable advice and discussions. I also thank Rob Ruigrok and Maïté Paternostre for helpful discussions and careful reading of the manuscript, Anne Flamand for constant interest, and Christine Maheu for virus purification.

This work was supported by the CNRS (UPR 9053).

Submitted: 18 April 2000
Revised: 19 June 2000
Accepted: 20 June 2000

References

Bagai, S., and R. Lamb. 1996. Truncation of the COOH-terminal region of the paramyxovirus SV5 fusion protein leads to hemifusion, but not complete fusion. *J. Cell Biol.* 135:73–84.

Baker, K.A., R.E. Dutch, R.A. Lamb, and T.S. Jardetzky. 1999. Structural basis for paramyxovirus-mediated membrane fusion. *Mol. Cell.* 3:309–319.

Blumenthal, R., D.P. Sarkar, S. Durell, D.E. Howard, and S.J. Morris. 1996. Dilation of the influenza hemagglutinin pore revealed by the kinetics of individual cell–cell fusion events. *J. Cell Biol.* 135:63–71.

Broring, K., C.W. Haest, and B. Deuticke. 1989. Translocation of oleic acid across the erythrocyte membrane. Evidence for a fast process. *Biochim. Biophys. Acta.* 986:321–331.

Bullough, P.A., F.M. Hughson, J.J. Skehel, and D.C. Wiley. 1994. Structure of influenza haemagglutinin at the pH of membrane fusion. *Nature.* 371:37–43.

Bundo-Morita, K., S. Gibson, and J. Lenard. 1988. Radiation inactivation analysis of fusion and hemolysis by vesicular stomatitis virus. *Virology.* 163:622–624.

Chan, D.C., D. Fass, J.M. Berger, and P.S. Kim. 1997. Core structure of gp41 from the HIV envelope glycoprotein. *Cell.* 89:263–273.

Chernomordik, L.V., S.S. Vogel, A. Sokoloff, H.O. Onaran, E.A. Leikina, and J. Zimmerberg. 1993. Lysolipids reversibly inhibit Ca(2+)-, GTP- and pH-dependent fusion of biological membranes. *FEBS Lett.* 318:71–76.

Chernomordik, L.V., M.M. Kozlov, and J. Zimmerberg. 1995. Lipids in biological membrane fusion. *J. Memb. Biol.* 146:1–14.

Chernomordik, L.V., E. Leikina, V. Frolov, P. Bronk, and J. Zimmerberg. 1997. An early stage of membrane fusion mediated by the low pH conformation of influenza hemagglutinin depends upon membrane lipids. *J. Cell Biol.* 136: 81–93.

Chernomordik, L.V., V.A. Frolov, E. Leikina, P. Bronk, and J. Zimmerberg. 1998. The pathway of membrane fusion catalyzed by influenza hemagglutinin: restriction of lipids, hemifusion, and lipidic fusion pore formation. *J. Cell Biol.* 140:1369–1382.

Chernomordik, L.V., E. Leikina, M.M. Kozlov, V.A. Frolov, and J. Zimmerberg. 1999. Structural intermediates in influenza haemagglutinin-mediated fusion. *Mol. Membr. Biol.* 16:33–42.

Clague, M.J., C. Schoch, L. Zech, and R. Blumenthal. 1990. Gating kinetics of pH-activated membrane fusion of vesicular stomatitis virus with cells: stopped-flow measurements by dequenching of octadecylrhodamine fluorescence. *Biochemistry.* 29:1303–1308.

Crimmins, D.L., W.B. Mehard, and S. Schlesinger. 1983. Physical properties of a soluble form of the glycoprotein of vesicular stomatitis virus at neutral and acidic pH. *Biochemistry.* 22:5790–5796.

Danieli, T., S.L. Pelletier, Y.I. Henis, and J.M. White. 1996. Membrane fusion mediated by the influenza virus hemagglutinin requires the concerted action of at least three hemagglutinin trimers. *J. Cell Biol.* 133:559–569.

Doms, R.W., D.S. Keller, A. Helenius, and W. Balch. 1987. Role for adenosine triphosphate in regulating the assembly and transport of vesicular stomatitis virus G protein trimers. *J. Cell Biol.* 105:1957–1969.

Durrer, P., Y. Gaudin, R.W.H. Ruigrok, R. Graf, and J. Brunner. 1995. Photolabeling identifies a putative fusion domain in the envelope glycoprotein of rabies and vesicular stomatitis viruses. *J. Biol. Chem.* 270:17575–17581.

Fass, D., S.C. Harrison, and P.S. Kim. 1996. Retrovirus envelope domain at 1.7 Å resolution. *Nat. Struct. Biol.* 3:465–469.

Fredericksen, B.L., and M.A. Whitt. 1995. Vesicular stomatitis virus glycoprotein mutations that affect membrane fusion activity and abolish virus infectivity. *J. Virol.* 69:1435–1443.

Fredericksen, B.L., and M.A. Whitt. 1996. Mutations at two conserved amino acids in the glycoprotein of vesicular stomatitis virus affect pH-dependent conformational changes and reduce the pH threshold for membrane fusion.

Virology. 217:49–57.

Fujii, T., A. Tamura, and T. Yamane. 1985. Trans-bilayer movement of added phosphatidylcholine and lysophosphatidylcholine species with various acyl chain lengths in plasma membrane of intact human erythrocytes. *J. Biochem*. 98:1221–1227.

Gaudin, Y. 2000. Reversibility in fusion protein conformational changes: the intriguing case of rhabdovirus-induced membrane fusion. *In* Subcellular Biochemistry: Fusion of Biological Membranes and Related Problems. H. Hilderson and S. Fuller, editors. Plenum Press, New York. 379–408.

Gaudin, Y., C. Tuffereau, D. Segretain, M. Knossow, and A. Flamand. 1991. Reversible conformational changes and fusion activity of rabies virus glycoprotein. *J. Virol.* 65:4853–4859.

Gaudin, Y., R.W.H. Ruigrok, C. Tuffereau, M. Knossow, and A. Flamand. 1992. Rabies virus glycoprotein is a trimer. *Virology*. 187:627–632.

Gaudin, Y., R.W.H. Ruigrok, M. Knossow, and A. Flamand. 1993. Low-pH conformational changes of rabies virus glycoprotein and their role in membrane fusion. *J. Virol.* 67:1365–1372.

Gaudin, Y., C. Tuffereau, P. Durrer, A. Flamand, and R.W.H. Ruigrok. 1995. Biological function of the low-pH, fusion-inactive conformation of rabies virus glycoprotein (G): G is transported in a fusion-inactive state-like conformation. *J. Virol.* 69:5528–5534.

Gaudin, Y., H. Raux, A. Flamand, and R.W.H. Ruigrok. 1996. Identification of amino acids controlling the low-pH-induced conformational change of rabies virus glycoprotein. *J. Virol.* 70:7371–7378.

Gaudin, Y., C. Tuffereau, P. Durrer, J. Brunner, A. Flamand, and R. Ruigrok. 1999. Rabies virus-induced membrane fusion. *Mol. Membr. Biol.* 16:21–31.

Günther-Ausborn, S., and T. Stegmann. 1997. How lysophosphatidylcholine inhibits cell–cell fusion mediated by the envelope glycoprotein of human immunodeficiency virus. *Virology*. 235:201–208.

Kemble, G.W., T. Danieli, and J.M. White. 1994. Lipid-anchored influenza hemagglutinin promotes hemifusion, not complete fusion. *Cell*. 76:383–391.

Kobe, B., R.J. Center, B.E. Kemp, and P. Poumbourios. 1999. Crystal structure of human T cell leukemia virus type 1 gp21 ectodomain crystallized as a maltose-binding protein chimera reveals structural evolution of retroviral transmembrane proteins. *Proc. Natl. Acad. Sci. USA*. 96:4319–4324.

Leikina, E., and L.V. Chernomordik. 2000. Reversible merger of membranes at the early stage of influenza hemagglutinin-mediated fusion. *Mol. Biol. Cell.* In press.

Li, Y., C. Drone, E. Sat, and H.P. Ghosh. 1993. Mutational analysis of the vesicular stomatitis virus glycoprotein G for membrane fusion domains. *J. Virol.* 67:4070–4077.

Lindau, M., and W. Almers. 1995. Structure and function of fusion pores in exocytosis and ectoplasmic membrane fusion. *Curr. Opin. Cell Biol.* 7:509–517.

Madden, T.D., and P.R. Cullis. 1982. Stabilization of bilayer structure for unsaturated phosphatidylethanolamines by detergents. *Biochim. Biophys. Acta.* 684:149–153.

Markovic, I., H. Pulyaeva, A. Sokoloff, and L.V. Chernomordik. 1998. Membrane fusion mediated by baculovirus gp64 involves assembly of stable gp64 trimers into multiprotein aggregates. *J. Cell Biol.* 143:1155–1166.

Melikyan, G.B., W.D. Niles, M.E. Peeples, and F.S. Cohen. 1993. Influenza hemagglutinin-mediated fusion pores connecting cells to planar membranes: flickering to final expansion. *J. Gen. Physiol.* 102:1131–1149.

Melikyan, G.B., W.D. Niles, V.A. Ratinov, M. Karhanek, J. Zimmerberg, and F.S. Cohen. 1995a. Comparison of transient and successful fusion pores connecting influenza hemagglutinin expressing cells to planar membranes. *J. Gen. Physiol.* 106:803–819.

Melikyan, G.B., J.M. White, and F.S. Cohen. 1995b. GPI-anchored influenza hemagglutinin induces hemifusion to both red blood cell and planar bilayer membranes. *J. Cell Biol.* 131:679–691.

Melikyan, G.B., S.A. Brener, D.C. Ok, and F.S. Cohen. 1997. Inner, but not outer, membrane leaflets control the transition from glycosylphosphatidylinositol-anchored influenza hemagglutinin-induced hemifusion to full fusion. *J. Cell Biol.* 136:995–1005.

Monck, J.R., and J.M. Fernandez. 1992. The exocytic fusion pore. *J. Cell Biol.* 119:1395–1404.

Pak, C.C., A. Puri, and R. Blumenthal. 1997. Conformational changes and fusion activity of vesicular stomatitis virus glycoprotein: [^{125}I]iodonaphtyl azide photolabeling studies in biological membranes. *Biochemistry*. 36:8890–8896.

Plonsky, I., and J. Zimmerberg. 1996. The initial fusion pore induced by baculovirus GP64 is large and forms quickly. *J. Cell Biol.* 135:1831–1839.

Puri, A., J. Winick, R.J. Lowry, D. Covell, O. Eidelman, A. Walter, and R. Blumenthal. 1988. Activation of vesicular stomatitis virus fusion with cells by pretreatment at low pH. *J. Biol. Chem*. 263:4749–4753.

Puri, A., S. Grimaldi, and R. Blumenthal. 1992. Role of viral envelope sialic acid in membrane fusion mediated by the vesicular stomatitis virus envelope glycoproteins. *Biochemistry*. 31:10108–10113.

Qiao, H., R.T. Armstrong, G.B. Melikyan, F.S. Cohen, and J.M. White. 1999. A specific point mutant at position 1 of the influenza hemagglutinin fusion peptide displays a hemifusion phenotype. *Mol. Biol. Cell.* 10:2759–2769.

Schoch, C., R. Blumenthal, and M.J. Clague. 1992. A long-lived state for influenza virus–erythrocyte complexes committed to fusion at neutral pH. *FEBS Lett.* 311:221–225.

Siegel, D.P. 1993. Energetic of intermediates in membrane fusion: comparison of stalk and inverted micellar intermediate mechanisms. *Biophys. J.* 65:2124–2140.

Skehel, J.J., and D.C. Wiley. 1998. Coiled coils in both intracellular vesicle and viral membrane fusion. *Cell.* 95:871–874.

Stegmann, T., J.M. Delfino, F.M. Richards, and A. Helenius. 1991. The HA2 subunit of influenza hemagglutinin inserts into the target membrane prior to fusion. *J. Biol. Chem*. 266:18404–18410.

Struck, D.C., D. Hoekstra, and R.E. Pagano. 1981. Use of resonance energy transfer to monitor membrane fusion. *Biochemistry*. 20:4093–4099.

Tse, F.W., A. Iwata, and W. Almers. 1993. Membrane flux through the pore formed by a fusogenic viral envelope protein during cell fusion. *J. Cell Biol.* 121:543–552.

Tsurudome, M., R. Glück, R. Graf, R. Falchetto, U. Schaller, and J. Brunner. 1992. Lipid interactions of the hemagglutinin HA2 NH_2-terminal segment during influenza virus-induced membrane fusion. *J. Biol. Chem*. 267:20225–20232.

Vogel, S.S., E.A. Leikina, and L.V. Chernomordik. 1993. Lysophosphatidylcholine reversibly arrests exocytosis and viral fusion at a stage between triggering and membrane merger. *J. Biol. Chem*. 268:25764–25768.

Weber, T., G. Paesold, R. Mischler, G. Semenza, and J. Brunner. 1994. Evidence for H^+-induced insertion of the influenza hemagglutinin HA2 N-terminal segment into the viral membrane. *J. Biol. Chem*. 269:18353–18358.

Weissenhorn, W., A. Dessen, S.C. Harrison, J.J. Skehel, and D.C. Wiley. 1997. Atomic structure of the ectodomain from HIV-1 gp41. *Nature.* 387:426–430.

Weissenhorn, W., A. Carfi, K.H. Lee, J.J. Skehel, and D.C. Wiley. 1998. Crystal structure of the Ebola virus membrane fusion subunit, Gp2, from the envelope glycoprotein ectodomain. *Mol. Cell.* 2:605–616.

Wharton, S.A., L.J. Calder, R.W.H. Ruigrok, J.J. Skehel, D.A. Steinhauer, and D.C. Wiley. 1995. Electron microscopy of antibody complexes of influenza virus haemagglutinin in the fusion pH conformation. *EMBO (Eur. Mol. Biol. Organ.) J.* 14:240–246.

Whitt, M.A., L. Buonocore, C. Prehaud, and J.K. Rose. 1991. Membrane fusion activity, oligomerization, and assembly of the rabies virus glycoprotein. *Virology*. 185:681–688.

Yeagle, P.L., F.T. Smith, J.E. Young, and T.D. Flanagan. 1994. Inhibition of membrane fusion by lysophosphatidylcholine. *Biochemistry*. 33:1820–1827.

Zhang, L., and H.P. Ghosh. 1994. Characterization of the putative fusogenic domain in vesicular stomatitis virus glycoprotein G. *J. Virol.* 68:2186–2193.

Zimmerberg, J.R., S.S. Vogel, and L.V. Chernomordik. 1993. Mechanisms of membrane fusion. *Annu. Rev. Biophys. Biomol. Struct.* 22:433–466.

Zimmerberg, J., R. Blumenthal, M. Curran, D. Sarkar, and S. Morris. 1994. Restricted movement of lipid and aqueous dyes through pores formed by influenza hemagglutinin during cell fusion. *J. Cell Biol.* 127:1885–1894.